

Multifocal Ischemic Brain Infarctions Secondary to Spontaneous Basilar Artery Occlusion in a Dog with Systemic Thromboembolic Disease

F. Salger, C. Stahl, M. Vandeveldel, A. Piersigilli, and D. Henke

A 6-year-old, male intact Chihuahua was presented to the Veterinary Teaching Hospital of the University of Bern after experiencing a single generalized seizure. The dog was hypothermic (rectal temperature, 36.1°C), obtunded and had a non-ambulatory tetraparesis. Postural reactions were reduced in all 4 limbs and a right-sided head tilt, a severely reduced menace response, delayed direct and consensual pupillary light reflexes, and bilaterally absent nasal sensation and corneal reflexes were present. Other cranial nerve reflexes and segmental spinal reflexes were considered normal, and no pain response was elicited on spinal palpation or by passive movement of the head and neck. The clinical findings were consistent with multifocal intracranial disease with involvement of the forebrain and brainstem.

There was regenerative anemia (hematocrit 0.33 L/L; reference range, 0.39–0.57 L/L, reticulocytes 209.6×10^9 /L; reference range, 10.9 – 111.0×10^9 /L), a neutrophilic left shift (band neutrophils 0.55×10^9 /L; reference range, 0.0 – 0.3×10^9 /L) without neutrophilia (8.31×10^9 /L; reference range, 3.0 – 11.5×10^9 /L) and lymphopenia (0.6×10^9 /L; reference range, 1.0 – 4.8×10^9 /L). Hypokalemia (3.71 mmol/L; reference range, 4.22–5.43 mmol/L), hypocalcemia (2.15 mmol/L; reference range, 2.42–2.85 mmol/L), hypocholesterolemia (2.89 mmol/L; reference range, 3.47–10.03 mmol/L), hypoproteinemia (48.4 g/L; reference range, 56.0–73.0 g/L), hypoalbuminemia (24.1 g/L; reference range, 30.0–40.5 g/L), a low serum creatinine concentration (29 μ mol/L; reference range, 52–117 μ mol/L), hyperbilirubinemia (21.3 μ mol/L; reference range, 0.5–3.9 μ mol/L), and increased activity of alanine aminotransferase (661 IU/L; reference range, 26–126 IU/L), alkaline phosphatase (251 IU/L; reference range, 9–132 IU/L), aspartate aminotransferase (343 IU/L; reference range, 22–76 IU/L), creatine kinase (781 IU/L;

Abbreviations:

ADC	apparent diffusion coefficient
BAO	basilar artery occlusion
CT	computed tomography
DWI	diffusion weighted images
FLAIR	fluid attenuation inversion recovery
HU	Hounsfield units
MRI	magnetic resonance imaging
TW1	T1-weighted
TW2	T2-weighted

; reference range, 64–400 IU/L), gamma-glutamyl transferase (19 IU/L; reference range, 1–7 IU/L), and glutamate dehydrogenase (45 IU/L; reference range, 2–10 IU/L) were present. Abnormalities were not noted on urinalysis and oscillometric blood pressure measurements were within normal limits. Right and left lateral thoracic radiographs revealed mild generalized cardiomegaly without evidence of congestive heart failure, minimal pleural effusion, and reduced abdominal detail. Abdominal ultrasound revealed mild anechoic fluid with signs of peritonitis and steatitis of the abdominal fat, hepatomegaly and mild bilateral pyelectasis. Abdominocentesis revealed a clear fluid with low total protein concentration (12 g/L), consistent with transudate.

Magnetic resonance imaging (MRI)^a of the brain revealed multifocal intra-axial, sharply delineated lesions, mainly affecting the gray matter in the cerebellar vermis, right brainstem, left thalamus, right caudate nucleus, and dorsolaterally in the area of the right parietal and occipital lobes without mass effect. These lesions were hyperintense on T2-weighted (T2W) and fluid attenuation recovery (FLAIR) sequences, and hypointense on T1-weighted (T1W) sequences with no contrast enhancement after intravenous administration of 0.15 mmol/kg gadodiamide^b and no evidence of hemorrhage on T2*-weighted (T2*W) gradient echo sequences (Figs 1A, 2A). The lesions were hyperintense on diffusion weighted images (DWI), and hypointense on the apparent diffusion coefficient (ADC) map, indicating restriction of diffusion (Figs 1B, 2B). No abnormality of the basilar artery was observed on conventional T1W and T2W spin echo, FLAIR, T2*W, and DWI MRI sequences, however, MR angiography was not performed. MRI findings were compatible with multifocal, acute, ischemic infarction.

Cerebrospinal fluid, collected from the cerebellomedullary cistern, contained 27 white blood cells per

From the Division of Neurological Sciences, (Salger, Vandeveldel, Henke); the Division of Clinical Neurology, (Salger, Vandeveldel, Henke); the Department of Clinical Veterinary Medicine, (Salger, Stahl, Vandeveldel, Henke); the Division of Clinical Radiology, (Stahl); and the Department of Veterinary Pathology, Vetsuisse Faculty, University of Bern, Bern, Switzerland (Piersigilli).

Corresponding author: F. Salger, Division of Neurological Sciences, Vetsuisse Faculty, University of Bern, 3012 Bern, Switzerland; e-mail: florian.salger@vetsuisse.unibe.ch.

Submitted March 28, 2014; Revised June 9, 2014; Accepted July 30, 2014.

Copyright © 2014 by the American College of Veterinary Internal Medicine

DOI: 10.1111/jvim.12447

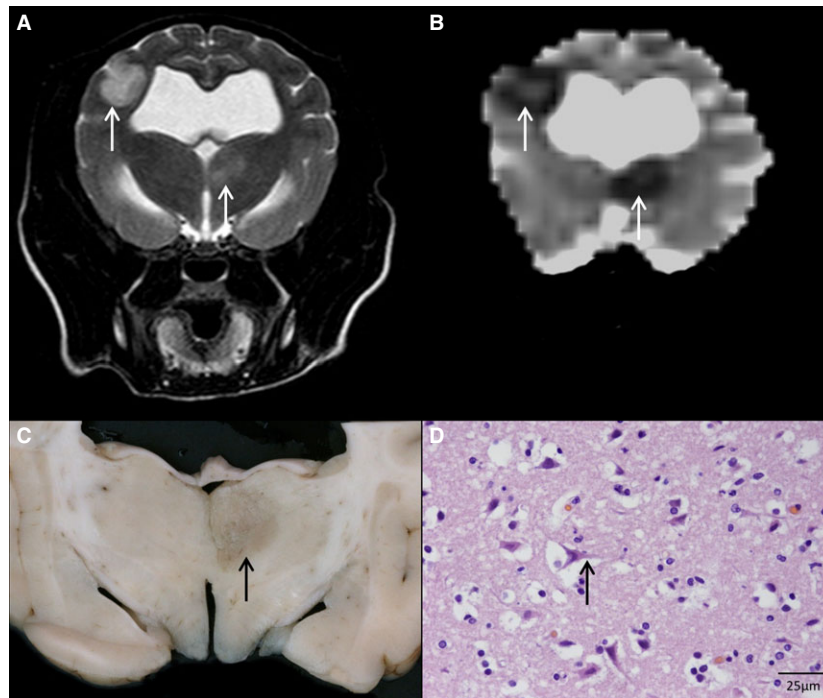


Fig 1. T2-weighted transverse MR image (A) at the level of the thalamus, showing T2-hyperintense, intra-axial, sharply delineated lesions, mainly affecting the gray matter of the left thalamus and right parietal lobe (arrows). The corresponding apparent diffusion coefficient map (B) shows restricted diffusion (arrows), compatible with acute, ischemic infarction. On gross pathology (C), a round, sharply demarcated, gray area is evident in the left thalamus (arrow). On histopathology (D), acidophilic neuronal necrosis of most of the neurons (arrow) and edematous neuropil within the affected areas are evident (H&E, 100 \times). [Color figure can be viewed in the online issue, which is available at wileyonlinelibrary.com.]

microliter (reference range, $<5/\mu\text{L}$), 30 mg/dL albumin (urine dipstick; reference range, <30 mg/dL), and a negative Pandy test (reference range, negative). Differential cell counts performed on cytospin preparations revealed 66% neutrophils, 27% monocytes, and 7% lymphocytes. This moderate, neutrophilic pleocytosis was consistent with the ischemic infarctions diagnosed on MRI. Results of a coagulation profile (partial thromboplastin time, prothrombin time) and thrombelastometry were within normal limits.

During the post-anesthetic phase, the dog developed cardiac arrhythmias (ventricular premature contractions) and dyspnea, which were soon followed by cardiac arrest. Attempts at resuscitation were unsuccessful and the dog was submitted for a complete necropsy.

Gross examination of the brain and spinal cord revealed bilateral, multifocal, round, sharply demarcated, gray areas of approximately 1 cm diameter in the dorsal areas of the caudate nuclei and thalamus (Fig 1C). The gray matter of the cortex was darkly discolored, especially in the right temporal lobe. No gross changes to the spinal cord were detected. Other gross examination findings included multiple bilateral acute renal infarcts, an approximately 0.5 cm area of myocardial necrosis at the intersection of the left ventricle and septum, diffuse hepatopathy and mild prostatomegaly.

Histopathologic examination of the brain revealed sharply demarcated areas of pale-staining tissue in the caudate nuclei, the thalamus, the cerebellar vermis, the

medial parts of the central cerebellar nuclei (Fig 2D) and brainstem, mostly affecting the ventral region and the reticular formation, bilaterally. In addition, most neurons in the cerebral cortex were shrunken and eosinophilic with pyknotic nuclei (acidophilic neuronal necrosis) (Fig 1D). The neuropil of affected regions was characterized by status spongiosus, attributed to edema, and infiltrated with few neutrophils and macrophages (Figs 1D, 2D). The lumen of the basilar artery was completely obliterated by an organized thromboembolus at the level of the medulla oblongata (Fig 2C). No other thromboemboli were found in the examined sections of the brain. The neurohistopathologic diagnosis was multiple ischemic infarctions and global brain ischemia caused by thromboembolism of the basilar artery.

Histopathologic examination of other organs revealed a renal thromboembolus causing complete obliteration of the interlobar artery (Fig 3A), multiple areas of coagulative necrosis with multifocal infiltration of neutrophils and hemorrhagic borders corresponding to the macroscopic areas of infarction (Fig 3A), and chronic tubulo-interstitial nephritis in the remaining tissue. In the region of gross myocardial necrosis, there were areas of myocardial fiber degeneration, coagulative necrosis, multifocal contraction bands, and were expanded by edema and infiltration with neutrophils and a few lymphocytes (Fig 3B), consistent with subacute myocardial infarction. A thromboembolus,

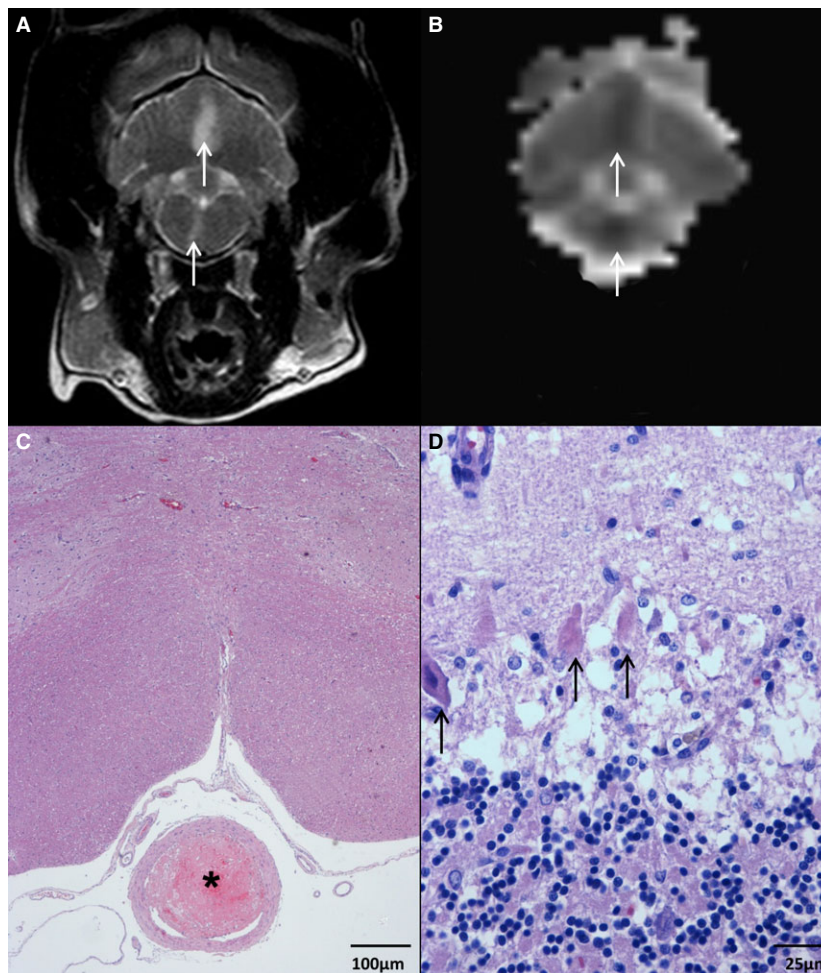


Fig 2. T2-weighted transverse MR image (A) at the level of the cerebellum and medulla oblongata, showing two T2-hyperintense, intra-axial, sharply delineated lesions, mainly affecting the gray matter in the cerebellar vermis and right brainstem (arrows). The corresponding apparent diffusion coefficient map (B) shows restricted diffusion (arrows), compatible with acute, ischemic infarctions. On histopathology (C), the lumen of the basilar artery is completely obliterated by an organized thromboembolus (asterisk) at this level (H&E, 40 \times). On histopathology of the cerebellar lesion (D), extensive acidophilic neuronal necrosis of the Purkinje cell layer (arrows) with marked edema of the surrounding neuropil are evident (H&E, 100 \times). [Color figure can be viewed in the online issue, which is available at wileyonlinelibrary.com.]

causing complete occlusion of the coronary artery, was present above the area of infarction (Fig 3C). In the liver, there was marked sinusoidal dilatation, predominantly in the centrilobular area, consistent with hepatic congestion, and intracanalicular bile plugs, consistent with hepatic cholestasis. In centrilobular areas, there was multifocal hepatocyte coagulative necrosis and venous luminal narrowing (up to 80%) by round cells of approximately 15–20 μm diameter with oval nuclei, finely stippled chromatin and moderate to abundant eosinophilic cytoplasm (Fig 3D). Cells infiltrating the vessel walls were CD3 (Mouse Monoclonal Antibody, LN10, 1 : 100)^c and CD20 (Rabbit Polyclonal Antibody, 1 : 800)^d positive lymphocytes and macrophages; the intraluminal cells were CD3, CD20, and MAC378 (Mouse Monoclonal Antibody, MAC 387, 1 : 4,000)^e negative but CD18 (Mouse Monoclonal Antibody, CA1.4E9, 1 : 30)^f positive, suggesting dendritic cells. However, the lack of frozen samples precluded any further characterization of these

cells. Based on these findings, the intraluminal changes were considered most likely reactive, although a round cell tumor could not be completely excluded. In the lungs, there was multifocal distension of the perivascular space (edema). No significant histopathologic abnormalities were observed in the stomach, intestines, spleen, bone marrow, or lymph nodes.

In people, the clinical presentation of basilar artery occlusion (BAO) ranges from mild transient clinical signs, such as vertigo and headache, to devastating strokes. Basilar artery occlusion accounts for about 1% of all strokes in people, and case fatality despite thrombolytic treatment is approximately 50%.^{1,2} In contrast to human medicine, the true prevalence of brain infarction in dogs remains unknown, and descriptions of multifocal infarcts are limited to a few case reports. One describes 3 sequential ischemic brain infarcts of unknown underlying cause; another describes multiple ischemic brain infarcts in 2 dogs infected with *Leishmania infantum*.^{3,4} In both reports,

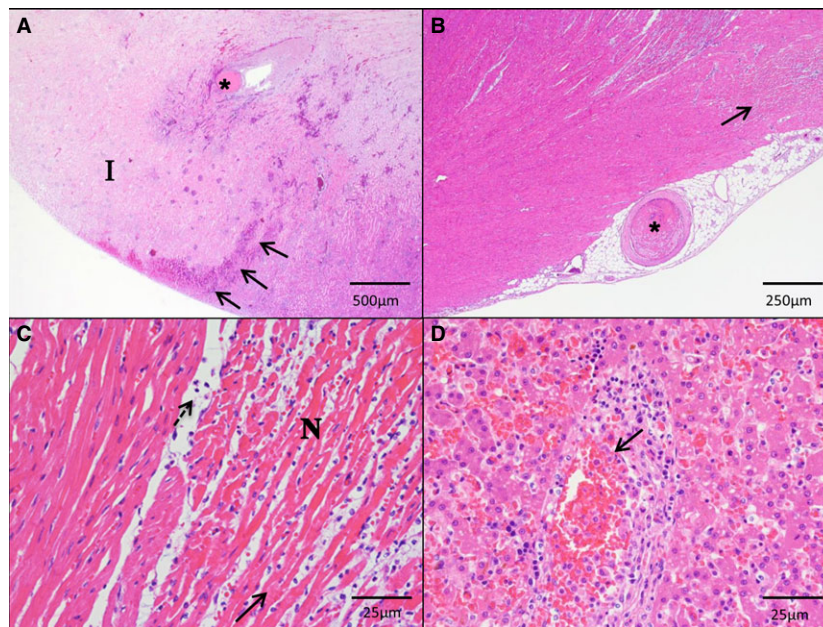


Fig 3. Histopathology of the kidney (A), showing a focal area of cortical ischemic tissue extending into the medulla (I) caused by complete obliteration of an interlobar artery (asterisk) by a thromboembolus. The arrows indicate the hemorrhagic borders of the infarction (H&E, 200 \times). Histopathology of the heart (B), showing the area of ischemic necrosis in the subepicardial myocardium (arrow) secondary to complete obliteration of the coronary artery lumen by a thromboembolus (asterisk) (H&E, 40 \times). Higher magnification (C) shows the necrotic myocardiocytes (N), characterized by hyper eosinophilia, loss of cytoplasmic details, and contraction bands (arrow), and the interstitium expanded by edema and infiltrating leukocytes (dashed arrow) (H&E, 400 \times). Histopathology of the liver (D), showing wall of the centrolobular vein infiltrated by few lymphocytes and macrophages. The lumen of the vessel is severely narrowed by an accumulation of round to oval eosinophilic cells (arrow), resembling dendritic cells (H&E, 400 \times). [Color figure can be viewed in the online issue, which is available at wileyonlinelibrary.com.]

infarction was restricted to the territory of striate and perforating arteries. Another report details the MRI findings in a dog with intravascular lymphoma resulting in multiple brain infarctions of different ages with thrombosis of the rostral cerebellar artery and other vessels.⁵ However, BAO was not described in these reports. In a study using the dog as an experimental model for the treatment of basilar artery thrombosis, approximately 50% of the dogs had single or multiple infarctions in the territory of the middle cerebral artery, thalamus, midbrain, or cerebellum on postmortem MRI.⁶ However, histopathologic examination was not performed in these dogs.

The blood supply to the cerebral arterial circle (circle of Willis) of the dog's brain has certain similarities to that in humans, but differs profoundly from that of other species, such as the ox, sheep and cat. In dogs and humans, the rostral parts of the brain are supplied by the internal carotid arteries (via the rostral and middle cerebral arteries), and the caudal parts of the brain are supplied by the basilar artery (via the caudal cerebral, rostral and caudal cerebellar arteries). Because of variations in blood supply to the circle of Willis and pressure gradients, blood flow in the basilar artery is caudal to rostral in dogs and humans but rostral to caudal in the cat, sheep, and ox.⁷ In addition, anastomoses derived from numerous branches of the external carotid artery contribute substantially to the cerebral arterial circle in dogs.⁸

In the case described herein, all areas of brain infarction were supplied by arteries almost exclusively receiving blood from the basilar artery: the parietal and occipital lobes, supplied by the caudal cerebral artery, the thalamus and basal ganglia, supplied by striate and perforating arteries of the caudal cerebral and caudal communicating artery, and the cerebellar vermis and brainstem, supplied by the rostral and caudal cerebellar arteries.^{9,10} Likewise, the clinical findings can be explained by a combination of focal lesions in these areas and concurrent global brain ischemia. Although not observed on histopathology, multiple thromboemboli in smaller brain arteries cannot be excluded. However, evidence of global brain ischemia suggests that multifocal brain infarction in this case is more likely caused by the embolic occlusion of the basilar artery alone. Moreover, this concurs with findings in people and experimental studies in dogs in which BAO often causes multifocal infarction, including in supra- and infratentorial areas.^{6,11} In people, a high number of infarcts is associated with a poor clinical outcome, as in the case reported herein.¹²

In general, ischemic infarction results from vascular obstruction from emboli originating in other vascular beds (artery-to-artery thromboembolism) or from the heart (cardioembolism), or from local thrombus formation within a vessel.¹³ The most frequent causes for BAO in humans are local atherosclerosis and embolic occlusions from cardiac and other large arteries.¹⁴ In

contrast to humans, both atherosclerosis and cardioembolic stroke are rare in dogs, although atherosclerosis has been associated with canine hypothyroidism and diabetes mellitus.¹⁵ There are, however, several underlying disorders associated with embolic stroke in dogs, including septic diseases (eg, endocarditis), parasites (eg, *Dirofilaria immitis*), primary or metastatic neoplasia, and fibrocartilaginous embolism.^{5,13,16–18} In one retrospective study, a concurrent medical condition was found in 18/33 (54%) of dogs with brain infarcts, of which chronic kidney disease and hyperadrenocorticism were the most common.¹⁹ In addition, approximately 30% of dogs with stroke were hypertensive, and a hypercoagulable state was suspected in around 10% of dogs.¹⁹ In the case described herein, atherosclerosis was excluded on histopathology. Hypothyroidism, hyperadrenocorticism, and diabetes mellitus were unlikely as typical clinical signs and clinicopathologic, imaging or pathologic findings were lacking. Hypertension was ruled out based on noninvasive arterial blood pressure measurements. Protein-losing nephropathy, associated with antithrombin loss, and chronic renal disease were unlikely based on the absence of azotemia and normal urinalysis. Decreased production of antithrombin caused by liver dysfunction cannot be ruled out, but is unlikely based on only moderate histopathologic parenchymal changes and unremarkable results of a coagulation panel and thrombelastometry. However, the latter may not be sensitive enough to exclude hyperaggregability of platelets.²⁰ Hepatic vein thrombosis with secondary coronary embolism is very unlikely as paradoxical embolism is only described in patients with cardiac septal defects.²¹ Moreover, pulmonary infarction or embolism were not observed, although emboli in small caliber vessels cannot be excluded as these are usually asymptomatic and can be missed on gross pathology. The hepatic centrilobular venous infiltration and narrowing may have led to thromboemboli both because of turbulent blood flow and phlebitis in this case.

Strokes have been increasingly identified over the last decade as the cause of acute neurologic signs in dogs by both MRI and computed tomography (CT).^{19,22–24} Whereas CT is particularly sensitive for detecting hemorrhagic infarction because of the difference in Hounsfield units (HU) of acute hemorrhage (56–76 HU) compared to gray (39 HU) or white (32 HU) matter, it is clearly inferior to MRI for the detection of ischemic infarction.²² Such lesions are typically well demarcated areas, preferentially involving the gray matter with minimal mass effect, which are hypointense on T1W, and hyperintense on T2W and FLAIR images, as was observed in the case described herein.²³ The lesions could be categorized as acute using DWI and ADC based on previously described imaging characteristics.²³ The occurrence of infarcts of similar age supports the theory that BAO was the likely underlying cause of multifocal infarction in this case. However, occlusion of the basilar artery was not detectable on pre- or post-contrast MRI sequences. This could be because BAO was not present at the

time of image acquisition or because BAO is simply not visible on MRI. In people, acute BAO can be diagnosed on CT or MR angiography, and digital subtraction angiography is considered the gold standard for the detection of BAO.¹⁴ The use of MR angiography has been described in dogs and could possibly have permitted an ante mortem diagnosis in our case.⁵

In summary, the clinical, MRI, and pathologic findings of this case reveal many similarities to those described for BAO in people and represent the first description of spontaneous BAO in the dog. The cause or origin of thromboembolism in this case was not evident. Although rare, BAO should be considered in dogs with suspected multiple brain infarcts and CT or MR angiography should be performed.

Footnotes

- ^a Phillips HFO 1.0T; Phillips Medical Systems, PC Best, The Netherlands
^b Omniscan; GE Healthcare, Munich, Germany
^c Novocastra, Newcastle-upon-Tyne, UK
^d Neomarkers, Fremont, CA
^e Dako, Glostrup, Denmark
^f Dr Peter Moore School of Veterinary Medicine, UC Davis, CA
-

Acknowledgments

The authors thank Dr Christine Göpfert from the Institute of Animal Pathology, University of Bern, Switzerland, and Nadine Isenschmid and Antonella Maggio from Pathologie Länggasse Bern, Bern, Switzerland for their help and technical support.

Conflict of Interest Declaration: The authors disclose no conflict of interest.

References

- Israeli-Korn SD, Schwammenthal Y, Yonash-Kimchi T, et al. Ischemic stroke due to acute basilar artery occlusion: Proportion and outcomes. *Isr Med Assoc J* 2010;12:671–675.
- Lindsberg PJ, Sairanen T, Strbian D, et al. Current treatment of basilar artery occlusion. *Ann N Y Acad Sci* 2012;1268:35–44.
- Major AC, Caine A, Rodriguez SB, Cherubini GBI. Imaging diagnosis—Magnetic resonance imaging findings in a dog with sequential brain infarction. *Vet Radiol Ultrasound* 2012;53:576–580.
- José-López R, la Fuente CD, Añor S. Presumed brain infarctions in two dogs with systemic leishmaniasis. *J Small Anim Pract* 2012;53:554–557.
- Kent M, Delahunta A, Tidwell AS. MR imaging findings in a dog with intravascular lymphoma in the brain. *Vet Radiol Ultrasound* 2001;42:504–510.
- Qureshi AI, Boulos AS, Hanel RA, et al. Randomized comparison of intra-arterial and intravenous thrombolysis in a canine model of acute basilar artery thrombosis. *Neuroradiology* 2004;46:988–995.
- King AS. Arterial supply to the central nervous system. In: King AS, ed. *Physiological and Clinical Anatomy of the Domes-*

tic Mammals: Central Nervous System, Volume 1. Oxford: Oxford University Press; 1987:1–12.

8. Jewell PA. The anastomoses between internal and external carotid circulations in the dog. *J Anat* 1952;86:83–94.

9. Garosi L, McConnell JF, Platt SR, et al. Clinical and topographic magnetic resonance characteristics of suspected brain infarction in 40 dogs. *J Vet Intern Med* 2006;20:311–321.

10. Vandeveld M. Vascular disorders. In: Vandeveld M, Higgins R, Oevermann A, eds. *Veterinary Neuropathology: Essentials of Theory and Practice*, 1st ed. Chichester, UK: John Wiley & Sons; 2012:38–47.

11. Caplan L, Chung CS, Wityk R, et al. New England medical center posterior circulation stroke registry: I. Methods, data base, distribution of brain lesions, stroke mechanisms, and outcomes. *J Clin Neurol* 2005;1:14–30.

12. Renard D, Landragin N, Robinson A, et al. MRI-based score for acute basilar artery thrombosis. *Cerebrovasc Dis* 2008;25:511–516.

13. Joseph RJ, Greenlee MS, Carillo JM, Kay WJ. Canine cerebrovascular disease: Clinical and pathological findings in 17 cases. *J Am Anim Hosp Assoc* 1988;24:569–576.

14. Mattle HP, Arnold M, Lindsberg PJ, et al. Basilar artery occlusion. *Lancet Neurol* 2011;10:1002–1014.

15. Hess RS, Kass PH, Van Winkle TJ. Association between diabetes mellitus, hypothyroidism or hyperadrenocorticism, and atherosclerosis in dogs. *J Vet Intern Med* 2003;17:489–494.

16. Cook LB, Coates JR, Dewey CW, et al. Vascular encephalopathy associated with bacterial endocarditis in four dogs. *J Am Anim Hosp Assoc* 2005;41:252–258.

17. Patton CS, Garner FM. Cerebral infarction caused by heartworms (*Dirofilaria immitis*) in a dog. *J Am Vet Med Assoc* 1970;156:600–605.

18. Axlund TW, Isaacs AM, Holland M, O'Brien DP. Fibrocartilaginous embolic encephalomyelopathy of the brainstem and midcervical spinal cord in a dog. *J Vet Intern Med* 2004;18:765–767.

19. Garosi L, McConnell JE, Platt SR, et al. Results of diagnostic investigations and long-term outcome of 33 dogs with brain infarction (2000–2004). *J Vet Intern Med* 2005;19:725–731.

20. Thawley VJ, Drobatz K, King L, Sanchez M. Association between results of thromboelastography (TEG) and post-mortem evidence of thromboembolism in critically ill dogs. *Vet Emerg Crit Care* 2012;22:S15. (abstract)

21. Mitchel RN. Hemodynamic disorders, thromboembolic disease, and shock. In: Kumar V, Abbas V, Fausto N, Asterr J, eds. *Robbins and Cotran Pathologic Basis of Disease*, 8th ed. Philadelphia, PA: Saunders Elsevier; 2010:125–127.

22. Paul AE, Lenard Z, Mansfield CS. Computed tomography diagnosis of eight dogs with brain infarction. *Aust Vet J* 2010;88:374–380.

23. McConnell JF, Garosi L, Platt SR. Magnetic resonance imaging findings of presumed cerebellar cerebrovascular accident in twelve dogs. *Vet Radiol Ultrasound* 2005;46:1–10.

24. Gredal H, Skerritt GC, Gideon P, et al. Spontaneous ischaemic stroke in dogs: Clinical topographic similarities to humans. *Acta Neurol Scand* 2013;128:11–16.